Mapping change of older forest with nearest-neighbor imputation and Landsat time-series

Janet L. Ohmann [a,*], Matthew J. Gregory [b], Heather M. Roberts [b], Warren B. Cohen [a], Robert E. Kennedy [b], Zhiqiang Yang [b]

[a] Pacific Northwest Research Station, USDA Forest Service, 3200 SW Jefferson Way, Corvallis, OR 97331, United States
[b] Department of Forest Ecosystems and Society, Oregon State University, Corvallis, OR 97331, United States

ABSTRACT

The Northwest Forest Plan (NWFP), which aims to conserve late-successional and old-growth forests (older forests) and associated species, established new policies on federal lands in the Pacific Northwest USA. As part of monitoring for the NWFP, we tested nearest-neighbor imputation for mapping change in older forest, defined by threshold values for forest attributes that vary with forest succession. We mapped forest conditions on >19 million ha of forest for the beginning (Time 1) and end (Time 2) of a 13-year period using gradient nearest neighbor (GNN) imputation. Reference data were basal area by species and size class from 17,000 forest inventory plots measured from 1993 to 2008. Spatial predictors were from Landsat time-series and GIS data on climate, topography, parent material, and location. The Landsat data were temporally normalized at the pixel level using LandTrendr algorithms, which minimized year-to-year spectral variability and provided seamless multi-scene mosaics. We mapped older forest change by spatially differencing the Time 1 and Time 2 GNN maps for average tree size (*MNDBH*) and for old-growth structure index (*OGSI*), a composite index of stand age, large live trees and snags, down wood, and diversity of tree sizes. Forests with higher values of *MNDBH* and *OGSI* occurred disproportionately on federal lands. Estimates of older forest area and change varied with definition. About 10% of forest at Time 2 had *OGSI* $\geq$50, with a net loss of about 4% over the period. Considered spatially, gross gain and gross loss of older forest were much greater than net change. As definition threshold value increased, absolute area of mapped change decreased, but increased as a percentage of older forest at Time 1. Pixel-level change was noisy, but change summarized to larger spatial units compared reasonably to known changes. Geographic patterns of older forest loss coincided with areas mapped as disturbed by LandTrendr, including large wildfires on federal lands and timber harvests on nonfederal lands. The GNN distribution of older forest attributes closely represented the range of variation observed from a systematic plot sample. Validation using expert image interpretation of an independent plot sample in TimeSync corroborated forest changes from GNN. An advantage of imputed maps is their flexibility for post-classification, summary, and rescaling to address a range of objectives. Our methods for characterizing forest conditions and dynamics over large regions, and for describing the reliability of the information, should help inform the debate over conservation and management of older forest.

Published by Elsevier B.V.

1. Introduction

The Northwest Forest Plan (NWFP) of 1994 aims to preserve late-successional and old-growth forests (henceforth "older forests") and associated species in the Pacific Northwest USA (USDA and USDI, 1994a). The NWFP instituted a major policy shift for federal land ownerships, including reduced harvesting of older forests and establishment of a reserve network (USDA and USDI, 1994b). Covering 9.3 million ha of federal forest within diverse ecoregions

spanning >23 million ha in Washington, Oregon, and California (Fig. 1), the NWFP represents one of the most sweeping landscape experiments in history.

The NWFP also implemented an Effectiveness Monitoring framework to track the status and trends of late-successional and old-growth forests, as well as watershed conditions, social and economic conditions, tribal relationships, and population and habitat for marbled murrelets and northern spotted owls. As a starting point for monitoring, NWFP documents define older forests only in general terms, as forest that meets structural, functional, or minimum age criteria (Hemstrom et al., 1998). Hemstrom et al. (1998) outlined an approach for monitoring older forests that involves
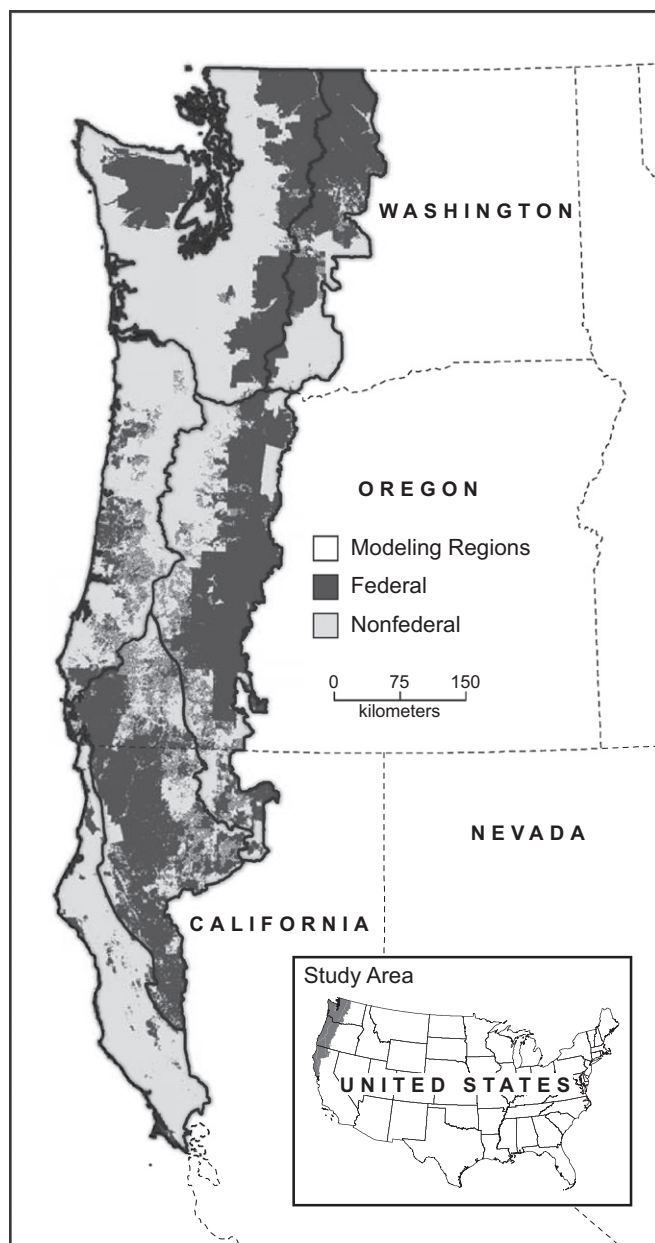
Fig. 1. Map of study area location, the area covered by the Northwest Forest Plan, showing modeling regions and land ownership.

complementary remote sensing (map-) and sample-based approaches while recognizing the need to adapt to advancements in technology and data. For remote sensing methods, they defined older forest as stands dominated by trees 50.8 cm (20 in.) diameter and larger, including both single- and multi-storied stands. While they recognized that sample-based approaches could consider more detailed elements of older forests, including live tree old-growth trees, standing dead trees, and fallen trees, no specific definitions were proposed.

The first monitoring assessment (Moeur et al., 2005) used satellite image classification to map broad forest classes at the beginning of the NWFP, and Landsat change detection methods to map stand-replacing disturbance as a basis of inferring losses of older forest over the 10-year period. They employed three definitions of older forest along a continuum based on average tree size and canopy layering. Their least restrictive definition, of "medium and large" forest, was based on a minimum average tree size of 50.8 cm (20 in.).

For the second (current) monitoring assessment (Moeur et al., 2011), which reports on the first 15 years of the NWFP, we sought methods for mapping forest conditions at both the beginning (Time 1) and end (Time 2) of the monitoring period, which could be used to assess change in older forest as well as wildlife habitat and watershed condition. Specifically, we looked to nearest-neighbor methods as a way to fill in missing data between forest inventory plots in both space (to make maps) and in time (to estimate change, or monitor). Our intent was to develop methods that also could be applied to monitoring change in older forest change into the future, as repeat measurement data become available. Monitoring results presented in the 15-year report (Moeur et al., 2011) were based on a simple definition of older forest chosen to be consistent with Hemstrom et al. (1998) and the first assessment (Moeur et al., 2005): stands with quadratic mean diameter of dominant and codominant conifers at least 50.8 cm (20 in.) and at least 10% canopy cover of conifers.

Nearest neighbor methods have become increasingly popular for mapping detailed forest characteristics over large areas (see reviews by Eskelson et al. (2009) and McRoberts et al. (2010)). In many applications, forest attributes from ground-based inventory plots are assigned to map locations where plot data are lacking. Usually there are less expensive predictor (X) variables available for all locations (such as from satellite imagery), but only a sample of locations where more detailed plot data (response (Y) variables) are available. The motivation behind nearest neighbor methods is that two locations with similar values for the spatial predictors should have similar values for the response variables.

Despite the growing use of nearest-neighbor methods internationally (see review by McRoberts et al. (2010)), we know of no applications to monitor change in detailed attributes of forest structure – and particularly for older forest – in a spatially explicit way. In the Pacific Northwest USA, we have used gradient nearest neighbor (GNN) imputation (Ohmann and Gregory, 2002) to map forest vegetation for a variety of forest ecosystems and objectives (Ohmann et al., 2007; Pierce et al., 2009; Ohmann et al., 2011), but only for a single map date. In this study, our objectives were to: (1) investigate GNN imputation for mapping forest vegetation at two dates; (2) use imputed maps to characterize change in the distribution of older forest attributes over the NWFP area; and (3) evaluate change estimates using newer methods for validation of multi-temporal map data.

In an analysis of the same GNN maps described in this paper, Moeur et al. (2011) assessed change in older forest using a simple, single definition of older forest. In this paper, we apply definitions of older forest that are more ecologically based and that consider multiple continuous attributes of forest structure, and examine the effect of varying the definition on the estimates of change in older forest area.

2. Methods

2.1. Study area

The NWFP area encompasses 23.2 million ha in the Pacific Northwest USA (Fig. 1), defined by the range of the northern spotted owl (*Strix occidentalis caurina*). 19.2 million ha within the region are forest land, of which 9.3 million ha (48%) are on federal lands covered by the NWFP (Forest Service, Bureau of Land Management, and National Park Service) (Moeur et al., 2011). Environmental gradients are shaped by the Pacific Ocean and by mountain ranges oriented mostly north-south. The climate is maritime along the Pacific Coast, with mild wet winters, cool dry summers, and heavy precipitation. Precipitation increases and temperature decreases from south to north. East of the crest of the Cascade

Mountains, temperatures fluctuate more widely and are more extreme, frost-free seasons are shorter and precipitation is much less. Except for lowland interior valleys, the region is dominated by mountainous terrain, with elevations ranging from sea level to >4,300 m, and coniferous forests. Broadleaf trees are associated with disturbed and wet sites, and become increasingly important in the mixed conifer and mixed evergreen forests of southwest Oregon and northwestern California. Fire is the predominant natural disturbance throughout the NWFP area, but in the last 100 years have been supplanted by timber management and wildfire suppression. For detailed descriptions of the vegetation, environment, and biogeography of the area (see Franklin and Dyrness (1988) and Barbour et al. (2007)).

2.2. GNN models for two dates

We mapped forest composition and structure across all forest land using GNN imputation as described in Ohmann and Gregory (2002) and Ohmann et al. (2011), with enhancements for two-date mapping aimed at minimizing differences between maps not associated with real change on the ground. Neighbor selection in GNN is based on weighted Euclidean distance within multivariate gradient space as determined from canonical correspondence analysis (CCA) (ter Braak, 1986), a method of constrained ordination (direct gradient analysis). We implemented GNN with $k = 1$, assigning a single nearest-neighbor plot to each map unit.

Spatial predictors (X variables) (Table 1) included climate variables derived from PRISM (Daly et al., 2008), which are 30-year normals, topographic and solar radiation variables derived from a 10-m-resolution digital elevation model, geographic location, and tasseled cap indices (Crist and Cicone, 1984) from Landsat imagery mosaics developed using LandTrendr algorithms (Kennedy et al., 2010). LandTrendr (Landsat Detection of Trends in Disturbance and Recovery) is a trajectory-based change detection method that simultaneously examines a time-series of yearly Landsat TM satellite images. Using images that are cloud-free, geometrically corrected, and radiometrically normalized (see Kennedy et al. (2010) for details), the LandTrendr algorithms identify segments of consistent trajectory for each pixel that describe sequences of disturbance and growth. The algorithms minimize annual variability from differences in sun angle, phenology, and atmospheric effects, such that the remaining signal more closely reflects real changes in vegetation. LandTrendr has thus far been used primarily to map forest disturbance and recovery, as was done for monitoring for

the NWFP (Moeur et al., 2011; Kennedy et al., in press). For this study, we used the resulting "temporally smoothed" imagery mosaics for Time 1 (1996 in Washington and Oregon, 1994 in California) and Time 2 (2006 in Washington and Oregon, 2007 in California) as spatial predictors in GNN. Because the LandTrendr algorithms accomplish normalization through time at the pixel level, multiple scenes can be mosaicked across large regions without incurring the obvious scene boundaries associated with traditional normalization and mosaicking processes.

Reference data (Y variables) were basal area by species and size class from 17,000 field plots measured from 1993 to 2008 in regional periodic and annual forest inventories: Forest Inventory and Analysis (FIA) Annual Inventory (USFS, 2003), FIA periodic inventories by USFS PNW and Region 5 (PNW-FIA Integrated Database version 2.0, http://www.fs.fed.us/pnw/fia/publications/data/data.shtml), Current Vegetation Survey (CVS) by USFS Region 6 and BLM (Max et al., 1996), and plots installed following the firemon protocol http://frames.nbii.gov/firemon/) in Josephine and Jackson Counties in southwest Oregon. At each plot location, there had been as many as three separate field measurements since 1990. Some were remeasurements using the same design, but others had somewhat different plot layouts and measurement protocols. We selected a single set of reference plots for use in all gradient modeling and imputation, to achieve geographic representation while minimizing effects of changing plot measurement protocols on resulting maps. For each plot location, we selected the single plot that was measured most closely to either the Time 1 or Time 2 imagery date. Plots measured in 2001 or later were matched to 2006 or 2007 imagery, and plots measured in 2000 or earlier were matched to 1994 or 1996 imagery. We excluded outlier plots, where field data did not match forest conditions in the imagery due to disturbance, inaccurate plot coordinates, or a distinct land cover boundary within the plot footprint. Previous analyses (unpublished data) have shown that excluding of outliers has minimal impact on results in terms of map accuracy, whereas retaining the outliers results in areas of egregious error (where an outlier plot is assigned as nearest neighbor) that map users strongly dislike.

We conducted gradient modeling and imputation for six large ecoregions (Fig. 1), at 30-m resolution. For each ecoregion, we developed a single CCA model using the selected plots within the ecoregion plus a 10-km buffer, which was then used in $k = 1$ imputation for both Time 1 and Time 2. Plots matched to Time 2 imagery could be selected as neighbors in the Time 1 imputation, and
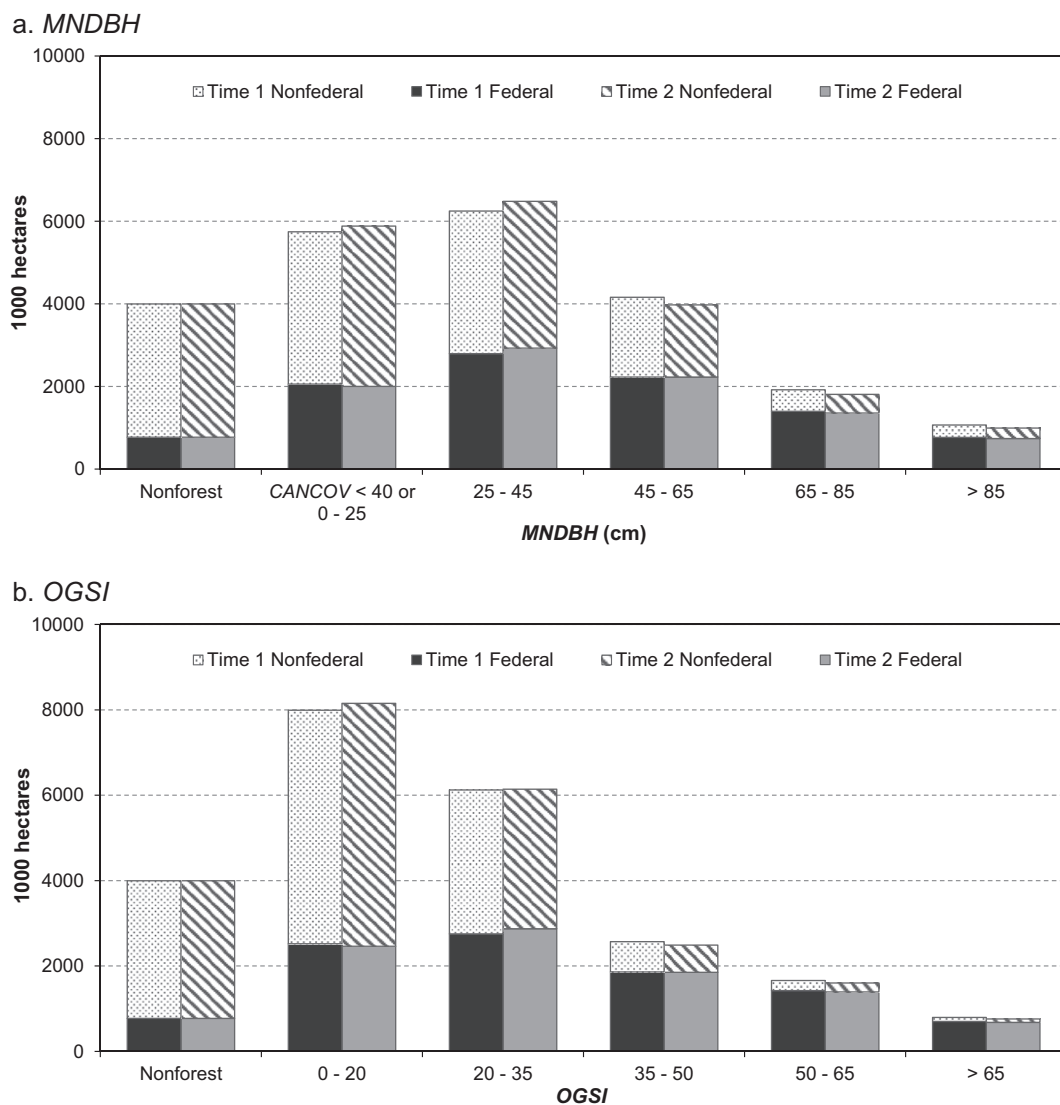
Table 1
Spatial predictors (X variables) used in CCA and GNN imputation.

Subset	Code	Description
Landsat TM	TC1	Axis 1 (brightness) from tasseled cap transformation, from LandTrendr (Kennedy et al., 2010) imagery
	TC2	Axis 2 (greenness) from tasseled cap transformation, from LandTrendr (Kennedy et al., 2010) imagery
	TC3	Axis 3 (wetness) from tasseled cap transformation, from LandTrendr (Kennedy et al., 2010) imagery
Climate	ANNPRE	Mean annual precipitation (natural logarithm, mm)
	ANNTMP	Mean annual temperature (°C)
	AUGMAXT	Mean maximum temperature of August (°C)
	CONTPRE	Percentage of annual precipitation falling during the growing season (June–August)
	DECMINT	Mean minimum temperature of (December) (°C)
	SMRTP	Growing season moisture stress, the ratio of mean temperature (°C) to precipitation (natural logarithm, mm), May–September
	STRATUS	Percentage of hours in July with cloud ceiling of marine stratus <1524 m and visibility <8 km. (unpubl. data from Chris Daly, resolution 795 m). (Oregon Coast only)
Topography	ELEV	Elevation (m)
	ASP	Cosine transformation of aspect (degrees)
	SOLAR	Cumulative potential relative radiation during the growing season (Pierce et al., 2005)
	SLOPE	Slope (%)
	TPI	Topographic position index, calculated as the difference between a cell's elevation and the mean elevation of cells within a 450-m-radius window
Substrate	SAND	Sandy sediments (categorical) (Oregon Coast only)
Location	UTME	Universal Transverse Mercator easting (m)
	UTMN	Universal Transverse Mercator northing (m)

Table 2
Forest attributes derived from tree-level data collected on field plots, used in characterizing older forest.

Forest attribute	Description
MNDBH	Mean conifer diameter at breast height (DBH) (cm), weighted by tree basal area, which emphasizes larger (overstory) trees
OGSI	Old-growth structure index (Spies et al., 2007), a composite index (0–100) based on AGEDOM, TPHC100, DDI, STPH5015, and DVPH
AGEDOM	Average field-recorded age (year) of all dominant and codominant trees (overstory) trees
TPHC100	Density (trees/ha) of all live conifers $\geqslant$100 cm DBH
DDI	Diameter diversity index, a measure of canopy structural diversity calculated from tree densities in four DBH classes (5–25, 25–50, 50–100, and >100 cm)
STPH5015	Density (trees/ha) of snags $\geqslant$50 cm DBH and $\geqslant$15 m tall
DVPH	Volume (m³/ha) of all down wood tallied
CANCOV	Canopy cover (percent) of all live trees, calculated from tree tally based on species, DBH, height, live crown ratio, and stand density using allometric equations

Fig. 2. Distribution of forest area by ownership and forest attribute (MNDBH (a) and OGSI (b)), at Time 1 and Time 2. CANCOV is total tree canopy cover (%).

vice versa. The validity of this approach relies on the assumption that LandTrendr effectively normalized the spectral values between image dates, i.e. that spectral values were equivalent in the two imagery years. As a result of these methods, all pixel-level differences in forest vegetation in the imputed GNN maps for Time 1 and Time 2 were associated with differences in the spectral data; all other X variables were held constant. Imputed ecoregion maps

were then mosaicked over the study area for Time 1 and Time 2. Nonforest areas were masked using land cover data from the USGS Gap Analysis Program (http://gapanalysis.nbii.gov/) and the National Land Cover Data set (NCLD) (http://landcover.usgs.gov/), and excluded from all analyses.

We mapped change in older forest attributes by differencing the GNN maps for Time 1 and Time 2. We had chosen to use k = 1 to
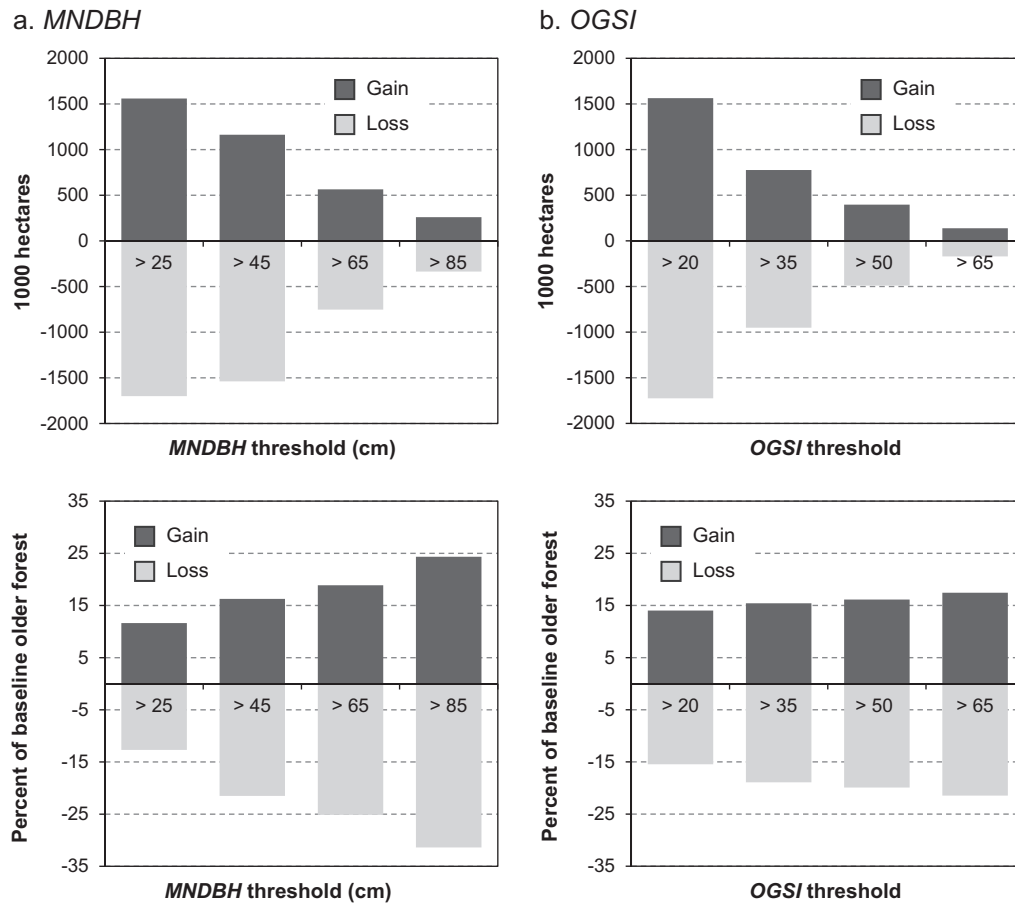
a. *MNDBH*

b. *OGSI*

Fig. 3. Change in distribution of older forest from Time 1 to Time 2, shown as gross gain and gross loss, by threshold value for *MNDBH* where *CANCOV* >40 (a) and *OGSI* (b). Change is expressed as area (top graphs) and as a percentage of older forest at Time 1 (bottom graphs).

maintain the covariance among multiple forest attributes within map units (pixels), an advantage for analyses where multiple attributes are to be analyzed together. For this study, we focused on two forest attributes that vary with forest development and succession and therefore are relevant to monitoring older forest: a simple metric based on average conifer size (*MNDBH*); and an old-growth structure index (*OGSI*) (Spies et al., 2007), a composite index based on stand age (*AGEDOM*), density of large conifers (*TPHC100*), diversity of tree sizes (*DDI*), density of large snags (*STPH5015*), and volume of down wood (*DVPH*) (Table 2). To map and estimate area of older forest, we defined older forest as pixels above a specified threshold value for *MNDBH* or *OGSI*. We also investigated the effect of varying this "definition threshold" on the estimates of older forest area. We chose a range of threshold values somewhat arbitrarily and primarily for illustration purposes. However, our threshold value of 50 for *OGSI* does correspond with the value used by Spies et al. (2007) in coastal Oregon to define late-successional and old-growth forest consistent with the NWFP. We preferred the *MNDBH* attribute of average tree size over alternative measures, such as the quadratic mean diameter of dominant and codominant trees used by Moeur et al. (2011), because it gives greater weight to larger trees while avoiding the subjective classifications of crown position by field crews. The *MNDBH* is almost always larger than the quadratic mean diameter for a given stand. Because of the large amount of forest in the study area with low density of large trees, due to either harsh site conditions or past disturbance, forest above a threshold value of *MNDBH* also had to have at least 40% canopy cover to be considered older forest.

Lastly, to reduce the effects of slight misregistrations between the two Landsat imagery dates, we filtered the Time 1 and Time 2 maps of *MNDBH* and *OGSI* using the focal median of a moving 3-by-3-pixel window. The 3-by-3-pixel approximates the footprint of the field plots, and median filtering tends to retain distinct boundaries between forest conditions.

2.3. Assessment of map reliability

To assess GNN map accuracy for older forest attributes at the local scale, we used modified leave-one-out cross-validation for all plots used in model development (Ohmann and Gregory, 2002). Because the Time 1 and Time 2 models were not independent (the same reference data were used in both models), the cross-validation assesses the reliability of both models and not the reliability of differences between models (i.e. change). Observed (field-measured) values were compared to predicted (map) values from the Time 1 or Time 2 model that was closest to year of plot measurement.

We also assessed model accuracy at the plot scale and for 8,660-ha hexagons (10-km spacing on center) using the protocol of Riemann et al. (2010). We compared imputed Time 2 map values to values from a systematic sample of *n* = 5,505 FIA Annual inventory plots, measured from 2001-2008. At the plot scale, we compared observed FIA plot values with GNN-predicted values for the 3-by-3-pixel windows coinciding with plot locations. Hexagon values were calculated as the means of the values for all plots in the hexagon, and the mean of all pixels within the 3-by-3-pixel
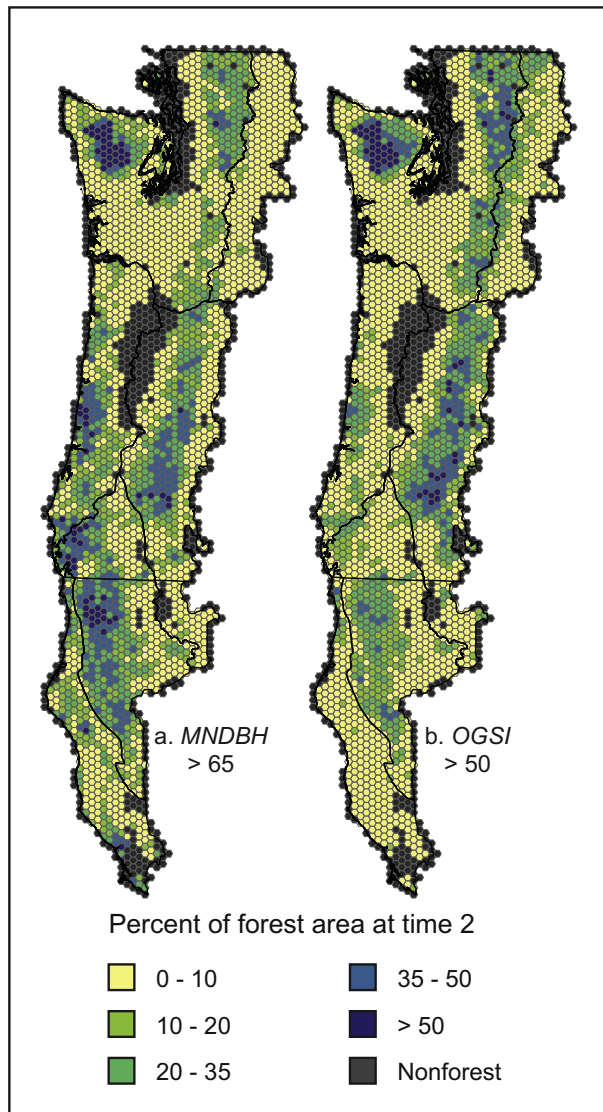
Fig. 4. Geographic distribution of older forest at Time 2 based on example threshold values for forest attributes: *MNDBH* ≥65 (a) and *OGSI* ≥50 (b). Values are percentage of GNN pixels meeting the threshold definition within 10-km hexagons.

plot footprints in the hexagon. From a scatterplot of predicted and observed values, we calculated the symmetric geometric mean functional relationship (GMFR) regression line (Ricker, 1984). Unlike least squares regression, the GMFR is a symmetric regression model that describes the relationship between two datasets that are both subject to error (see Riemann et al. (2010) for more detail). We constructed empirical cumulative distribution functions (ECDFs) for the plot- and GNN-based estimates as a way of comparing two distributions over larger geographic regions. We conducted these analyses for 30- and 50-km hexagons as well, but present only the 10-km results for brevity.

2.4. TimeSync validation of spatially explicit change estimates

To validate change in forest attributes between the Time 1 and Time 2 models in a spatially explicit way, i.e. to assess reliability of change at specific locations rather than change in area estimates summarized over larger regions, we adapted the TimeSync tool (Cohen et al., 2010). TimeSync was developed specifically for validating models based on Landsat time-series data, because independent validation plot data do not exist for assessing

multi-temporal models. TimeSync relies on expert interpretation of plots within the TimeSync user interface, which consists of four components: (1) a chip window, within which an area of user-defined size around an area of interest (i.e. plot) is displayed as a time-series of Landsat image chips, which are viewed simultaneously; (2) a trajectory window that displays the plot's spectral properties as a graphed trajectory of Landsat band reflectance or index through time; (3) a Google Earth window where a recent high-resolution image of the plot and its neighborhood, as well as historical imagery where available, can be viewed for context; and (4) an Access database window where the interpreter's observations about plot are entered. See Cohen et al. (2010) for more detail about TimeSync. The TimeSync interpretations have been demonstrated, through the use of existing reference data (e.g. field, airphoto, or other mapped data) where they do exist, to reliably capture disturbances that are visible in the forest canopy (Cohen et al., 2010). Disturbances in the understory (e.g., pre-commercial harvest or understory burning) cannot be seen in TimeSync.

For our application of TimeSync, we randomly selected $n = 570$ validation plots from strata defined by modeling region (Fig. 1) and by classes of GNN map attributes that describe successional status and change: *MNDBH* at Time 1, and the change in this variable from Time 1 to Time 2. The stratification assured an adequate sample of areas of change, particularly disturbed areas, which occupy a small proportion of the overall landscape. The interpreter examined each 3-by-3-pixel plot within TimeSync using the same Landsat time-series used in the LandTrendr algorithms, and within the context of current and historical aerial photography. Each plot was classified into one of five change categories that described events over the monitoring period: disturbed (high-, medium-, or low-severity), stable (no disturbance or recovery visible), or recovery (forest regrowth clearly visible). Disturbance severity classes were defined by loss of vegetation cover from Time 1 to Time 2: loss of <1/3 of Time 1 cover (low), 1/3–2/3 (medium), or >2/3 (high) (Cohen et al., 2010). Plots often contained multiple change classes, and the recorded trends described the average across the nine pixels. In cases where the monitoring period encompassed a disturbance event followed by regrowth, the interpreter assigned the change class based on net change in cover between Time 1 and Time 2.

For all of the validation plots within each of the five change categories interpreted in TimeSync, we summarized the change in total tree basal area between Time 1 and Time 2 by tree size (diameter at breast height, DBH), using values from tree-level data in the GNN-imputed pixels within each plot at Time 1 and Time 2.

3. Results and discussion

3.1. The changing distribution of older forest

At both Time 1 and Time 2, forests with lower values for the *OGSI* index of older forest structure occurred predominantly on nonfederal lands, whereas higher index values occurred disproportionately on federal lands (Fig. 2). Estimates of the amount of older forest varied as a function of the threshold value chosen to define older forest (Fig. 2). For example, at Time 2 about 12% of all forest land had *OGSI* ≥50, and 88% of it was on federal lands. There was a net loss of about 4% of older forest based on this definition threshold, where net change was determined aspatially as the difference between area estimates for Time 1 and Time 2 (Fig. 2). Patterns were similar for *MNDBH*. At Time 2, about 15% of forest land had *MNDBH* ≥65, and 75% of it was on federal lands. Based on this definition threshold, there was a net loss of about 6% of older forest.

When spatially differenced, the gross gain and gross loss of older forest were substantially greater than the net change in area (Fig. 3). This was true for both forest attributes and for all threshold
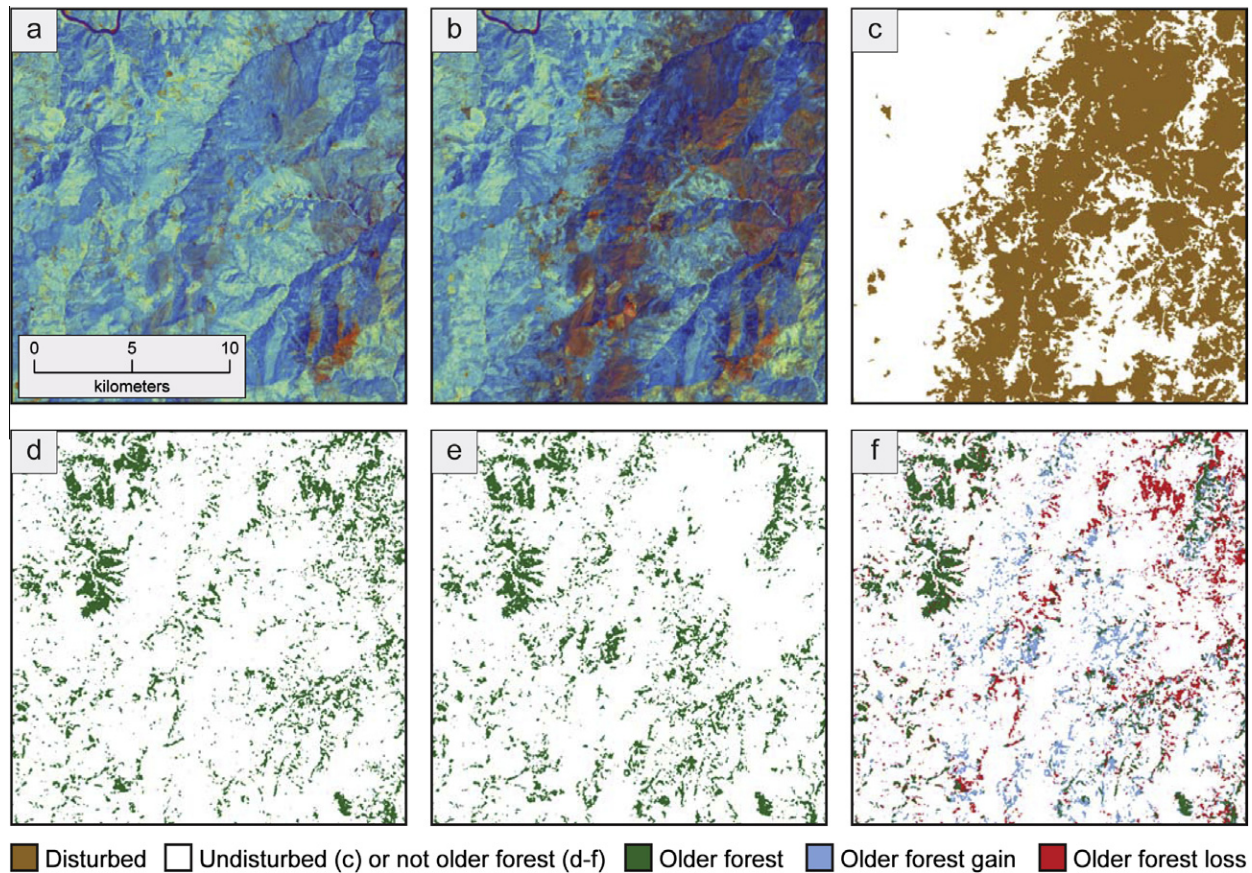
Disturbed ▢ Undisturbed (c) or not older forest (d-f) ■ Older forest ■ Older forest gain ■ Older forest loss

Fig. 5. A forest landscape in southwest Oregon encompassing a portion of the 2002 Biscuit Fire, showing tasseled cap axes 1–3 from Landsat imagery as a red-green-blue composite image for Time 1 (a) and Time 2 (b), areas mapped as disturbed from LandTrendr algorithms (c), older forest (*OGSI* ⩾ 50) from GNN at Time 1 (d) and Time 2 (e), and change in older forest from spatial differencing the Time 1 and Time 2 maps (f). Note the fine-scale variability in older forest as mapped by GNN, and the comingled areas of older forest gain and loss within the disturbed area.

values. As threshold value increased, the area (hectares) of mapped change decreased. However, at increasing threshold values the amount of change represented an increasing percentage of the area of older forest at Time 1 (Fig. 3). When expressed as a percentage of older forest at Time 1, gross gain and gross loss of older forest were more strongly affected by threshold value for *MNDBH* than for *OGSI*. In other words, *OGSI* appeared more stable (less noisy) over time, and therefore potentially more desirable for mapping change, possibly because it is based on multiple attributes rather than a single attribute.

The geographic distributions of older forest at Time 2 based on the above thresholds for *MNDBH* and *OGSI* were very similar overall when summarized to the spatial resolution of 10-km hexagons (Fig. 4), although some differences were apparent. For example, a greater percentage of forest met the older forest threshold for *MNDBH* than for *OGSI* in coastal and southwestern Oregon and California. Conversely, in much of the Washington and Oregon Cascades, in the eastern portions of the study area, a greater percentage of forest met the *OGSI* threshold. These patterns suggest that productive coastal forests may contain ample numbers of large live trees, which may develop at younger stand ages and lack the development of multi-layered canopies or large dead wood seen in the Cascades.

Although pixel-level change within local areas typically was noisy (Fig. 5), as expected from differencing two maps imputed with *k* = 1, when summarized to larger spatial units (10-km hexagons) the geographic patterns were quite reasonable and interpretable. Areas of major disturbance events (large wildfires and timber

harvest) were clearly visible, as were areas dominated by forest regrowth (Fig. 6). Areas of loss of older forest generally coincided with areas mapped as disturbed over the same period using LandTrendr (Kennedy et al., in press) (Fig. 6). This was particularly true for areas burned in large wildfires (Fig. 6d), which predominantly affected federal lands (Moeur et al., 2011). Older forest also decreased in areas where timber harvest was the dominant disturbance, almost exclusively on nonfederal ownerships (Moeur et al., 2011). Many hexagons dominated by harvest disturbance did not coincide with older forest loss or were mapped as older forest gain. This would be expected in landscapes where harvested stands were below the older forest threshold values for *MNDBH* and *OGSI* at Time 1. The LandTrendr algorithms identify disturbances but do not characterize the pre- and post-disturbance conditions of the disturbed forest.

3.2. Map reliability at local (plot), 10-km hexagon, and regional scales

Prediction accuracy (root mean squared error, RMSE) from cross-validation was slightly better at the scale of 10-km hexagons than at the plot scale for both of the older forest attributes (Fig. 7). Although the RMSEs for *OGSI* for *MNDBH* were comparable, the geometric mean functional relationship (GMFR) line for *OGSI* more closely matched the 1:1 line. The cross validation results apply equally to the Time 1 and Time 2 GNN maps.

The classification accuracy for older forest (vs. not older forest) will vary with the threshold value applied, by differentially affecting the sensitivity and specificity of the spatial predictions, as
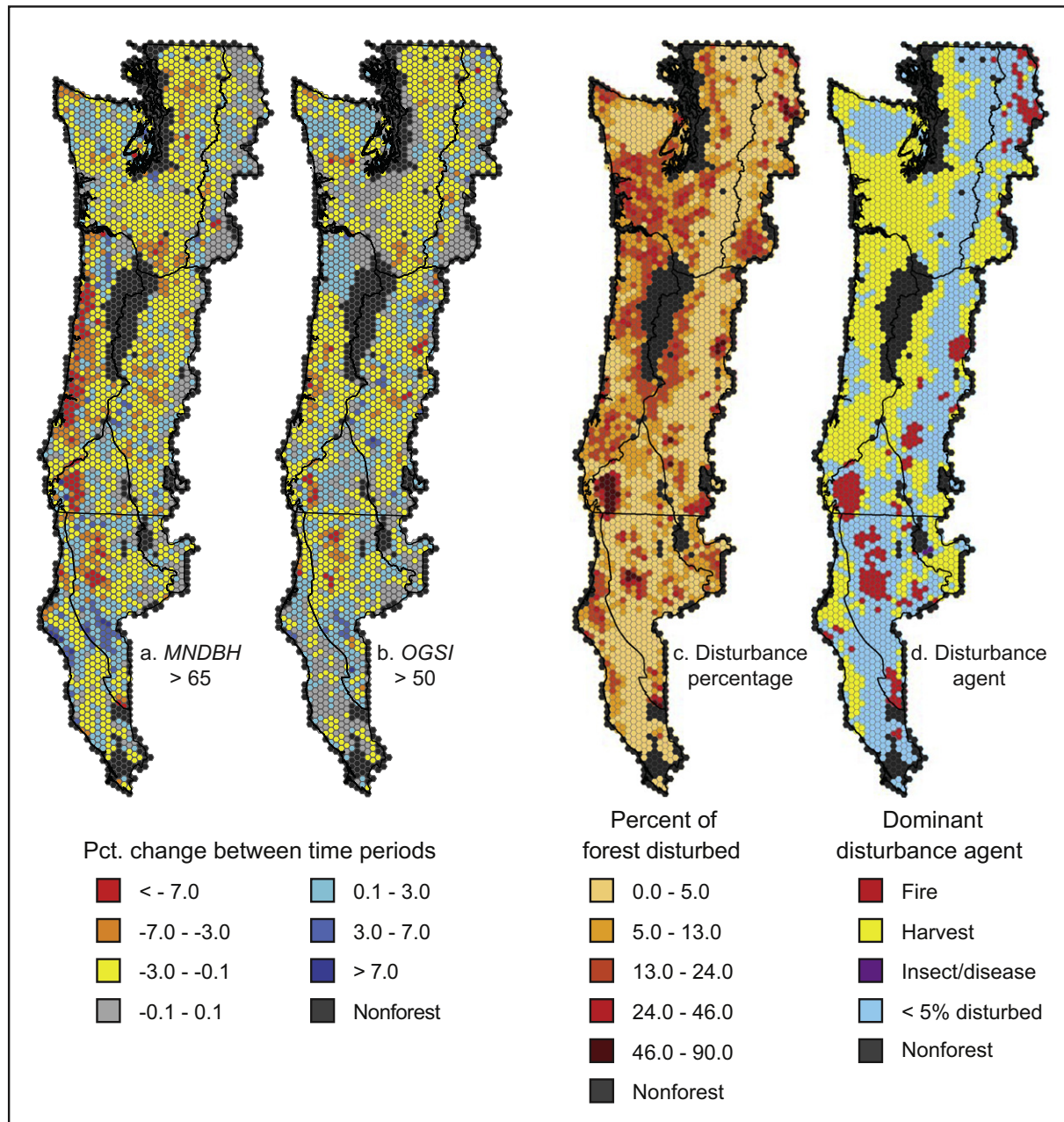
Fig. 6. Geographic distribution of forest change between Time 1 and Time 2: (a) Change in older forest (*MNDBH* ⩾65) from Time 1 to Time 2 (from GNN). (b) Change in older forest (*OGSI* ⩾50) (from GNN). (c) Percentage of forest disturbed (from LandTrendr; Kennedy et al., in press). (d) Dominant disturbance agent for hexagons with ⩾5% disturbance (from LandTrendr).

demonstrated by Chen et al. (2006). With imputed maps, the overall accuracy, sensitivity, and specificity are readily post-calculated for any threshold value of interest (see Moeur et al. (2011), Table 9, for one example), and map users may wish to consider these error rates in choosing a threshold value.

The empirical cumulative distribution functions (ECDFs) for the FIA plots and the Time 2 GNN map were quite similar for both older forest attributes and at both scales (Fig. 8). In all cases, the ECDFs indicated that the GNN maps very closely represented the distribution and range of variation in forest conditions present in the FIA plot sample. This is an important consideration when forest structure maps are used for spatially explicit ecosystem modeling (Duane et al., 2010), as is the case for the maps developed in this study (Moeur et al., 2011).

3.3. TimeSync validation of spatially explicit change between two GNN maps

The TimeSync validation data based on independent observations generally corroborated forest changes captured by the GNN maps for Time 1 and Time 2 (Fig. 9). On average, plots interpreted as one of the disturbance categories decreased in basal area from Time 1 to Time 2 from GNN, and the magnitude of basal area loss was positively correlated with disturbance severity. For areas of high- and medium-severity disturbance, almost all diameter classes decreased in basal area over the period. For low-severity disturbances, basal area of larger trees decreased but basal area of smaller trees increased, which likely could be attributed to post-disturbance regrowth of smaller trees within the monitoring
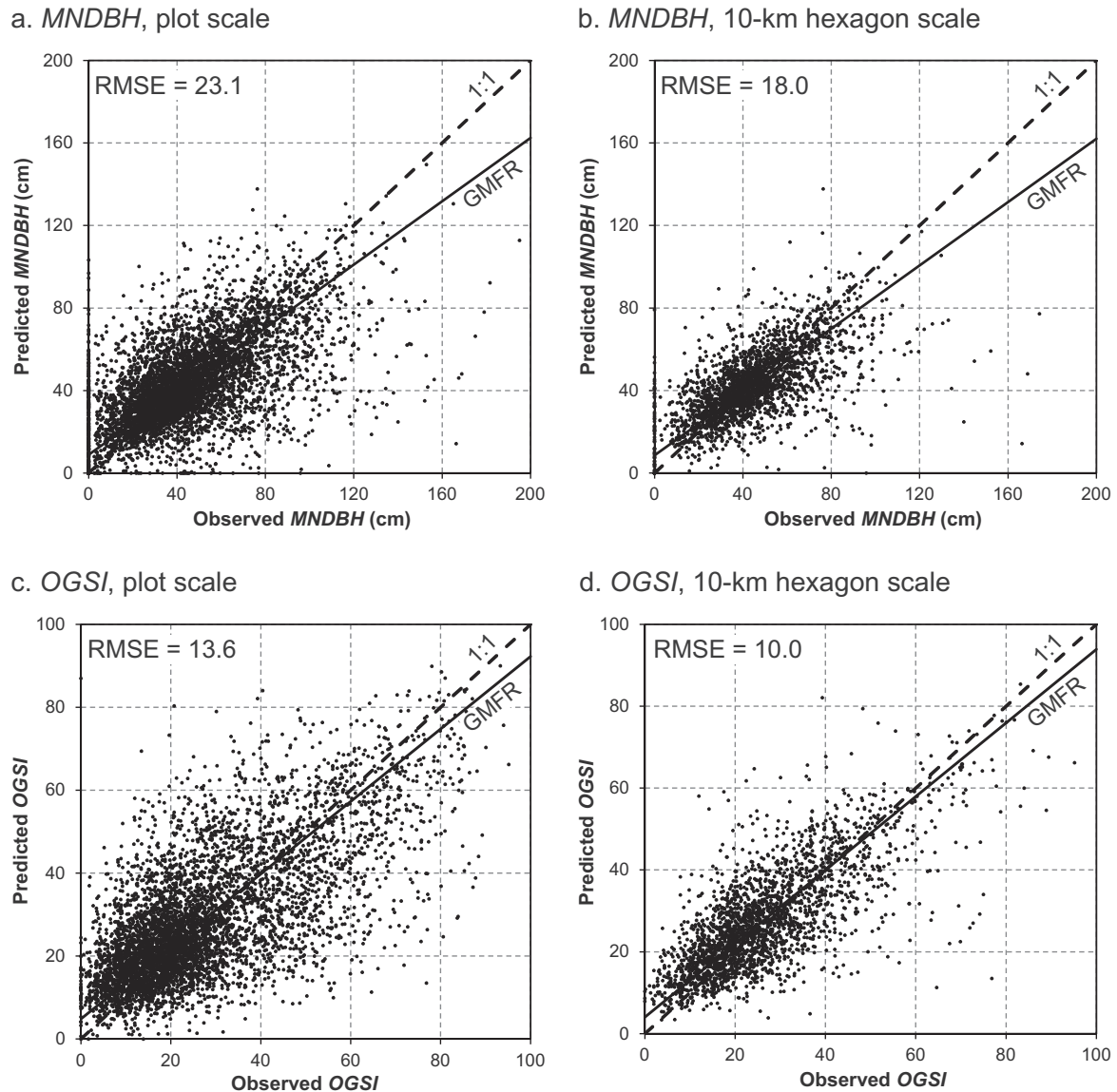
Fig. 7. Scatterplot of observed (plot) and predicted (from GNN) values at the plot and 10-km-hexagon scales, for *MNDBH* and *OGSI*. GMFR is the geometric mean functional relationship regression line, and RMSE is the root mean squared error.

period. Areas interpreted as stable showed very small amounts of both gain and loss in basal area across all diameter classes, probably an indication of fine-scale error in the GNN maps (Fig. 5) as well as natural variability among forests in this state. In areas interpreted as recovery, basal area increased in the smaller diameter classes as would be expected, while basal area change in the larger diameter classes was minor and variable. Basal area gain above 50 cm DBH was essentially nonexistent in any of the change categories.

3.4. Implications for spatial monitoring of landscape change with nearest-neighbor methods

Spatial monitoring of landscape dynamics poses unique challenges for model-based mapping. Our approach draws on the advantages of three newer methods: (1) The LandTrendr algorithms (Kennedy et al., 2010) normalize imagery through time at the pixel scale, which provides *X* variables for spatial modeling that are more stable spectrally through time for a given location than is possible with other normalization methods. The LandTrendr algo-

rithms also yield mosaics that are more consistent and seamless across multiple Landsat scenes than are obtained with other methods. (2) Nearest-neighbor imputation provides a means of characterizing forest pixels or patches with detailed attributes of forest composition and structure, which is not achieved with traditional change detection techniques that identify areas of change but little about the specific forest conditions. (3) TimeSync affords an accurate and independent assessment tool for characterizing errors in maps of forest change. In addition, we developed a novel way of combining multiple plot datasets that span a variety of date ranges into a single reference dataset for multi-date mapping. This approach would not be possible without the temporally normalized LandTrendr imagery. Taken together, these methods provide capability to map forest condition for any year, and at any time-step, for which imagery are available, not just for two dates as presented in this paper. In addition, our methods have the potential to be applied to other forest systems where both plot data and Landsat (or other imagery) time-series are available.

Results from this first investigation of nearest-neighbor imputation to map forest change are promising, but further improvements
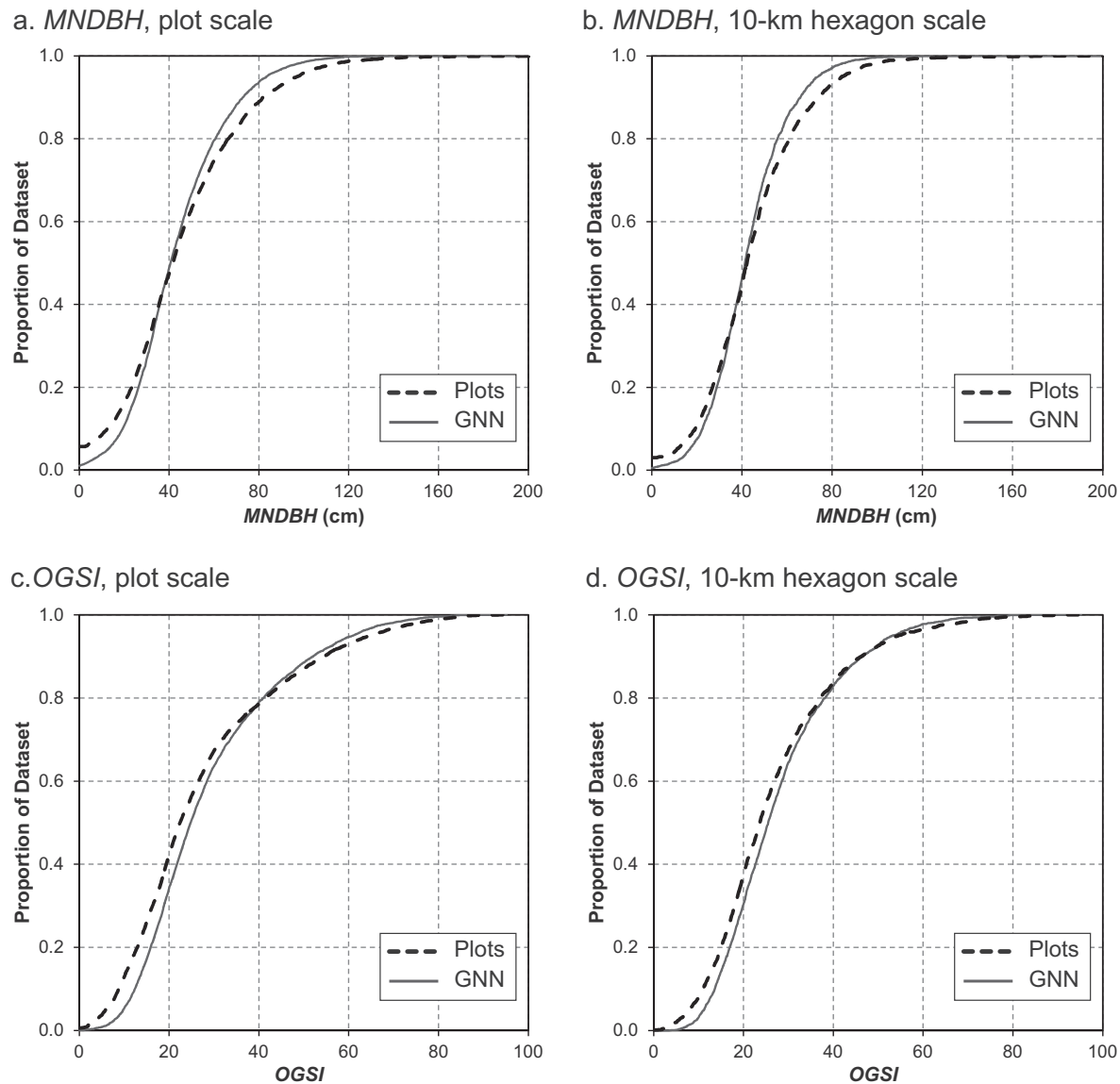
Fig. 8. Empirical cumulative distribution functions (ECDFs) for the FIA plot- and GNN-based estimates at the plot and 10-km-hexagon scales, for *MNDBH* and *OGSI*. The *n* = 5,505 FIA plots were measured from 2001 to 2008 and the GNN distributions are for Time 2 (2006/2007).

are needed. In particular, additional diagnostics are needed for describing the reliability of change information from model-based maps. In this study, the magnitude of estimated net change in older forest area was quite small relative to the various sources of error and uncertainty in the imputed maps. This could be attributed in part to the length of the monitoring period (10–13 years), which is quite short relative to the time needed for development of late-successional or old-growth characteristics (several decades to centuries). Nevertheless, we would like to be able to estimate the uncertainty of area estimates in the form of variances or standard errors, in order to state whether differences between two model-based estimates – in this case for two points in time – are statistically different. Approaches for variance estimation for *k*NN have only very recently been proposed (McRoberts et al., 2007; Magnussen et al., 2010; McRoberts et al., 2012) but are computationally intensive and have not yet been implemented over large study areas like ours.

Even if variance estimators were available, both developers and users of nearest-neighbor maps also would like to have information about the reliability of the spatially explicit (mapped) change

between two imputed maps. This is why we tested the new TimeSync validation procedure (Cohen et al., 2010), which was developed specifically for the purpose of validating maps of forest disturbance and regrowth. We successfully used TimeSync to corroborate the spatially explicit information on forest disturbance and growth contained in the GNN maps for Time 1 and Time 2. However, TimeSync cannot provide a true validation of a classification of older forest in the classic sense, because precise thresholds associated with class boundaries (e.g., *MNDBH* ≥65 or *OGSI* ≥50) cannot be reliably interpreted in Landsat imagery. Rather, the approach provides corroboration of GNN-based change estimates from a set of independent observations. Another limitation is that TimeSync validation results are aspatial, for a sample of plots, and do not depict error in a spatially explicit way.

In this study, where we imputed forest attributes at the 30-m pixel scale with *k* = 1, it is not surprising that the Time 1 and Time 2 maps contained a high level of fine-scale variability among pixels (Fig. 5). This variability was even more pronounced in the maps of forest change, constructed by spatially differencing two maps. Evidence suggested that much of the fine-scale
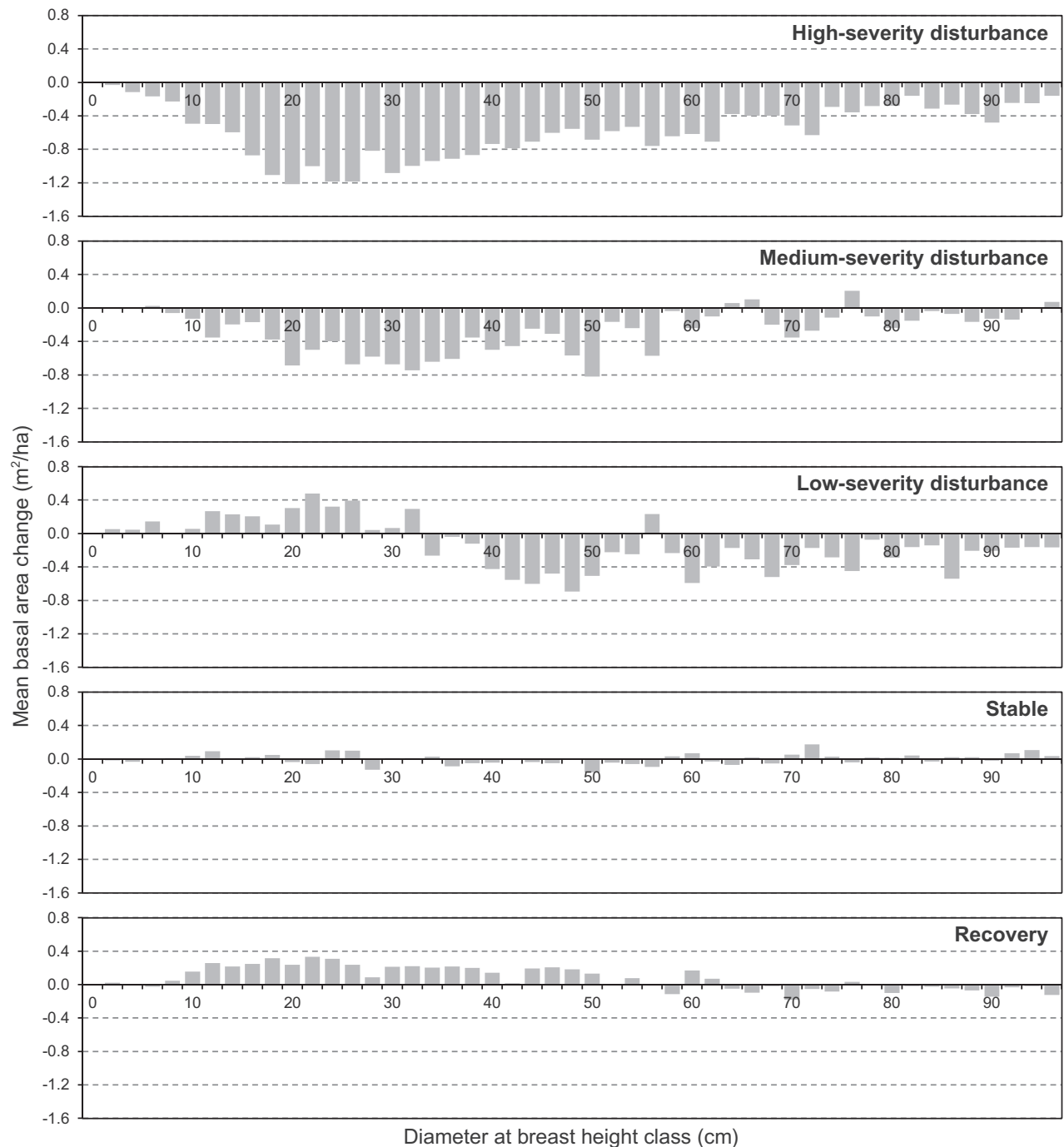
Fig. 9. Change in basal area between Time 1 and Time 2 by tree diameter class, using values for the GNN-imputed pixels within each of $n = 570$ validation plots at Time 1 and Time 2, by change classes interpreted in TimeSync. Basal area change is the difference between means at Time 1 and Time 2 of trees in the diameter class.

change in the maps was error rather than real change. This was indicated by the improvement in RMSEs at the 10-km-hexagon scale over the plot scale (Fig. 7), and by the fact that gross losses and gains of older forest greatly exceeded the amount of net change regardless of the threshold applied (Fig. 3). Yet despite the fine-scale noisiness (Fig. 5) and the lower prediction accuracy (RMSE) at the local scale (Fig. 7), the mapped distributions of older forest across the study area were very consistent with the FIA field plots at both the plot and 10-km-hexagon scales (Fig. 8). Estimates of older forest change from GNN also were corroborated by plot-based estimates from successive forest inventories where available, as reported by Moeur et al. (2011)

based on analyses of the same GNN maps. Furthermore, geographic patterns of older forest and change were consistent with mapped disturbances over the same period (Fig. 6).

The primary challenge of this study, as with any model-based estimation, was to reduce error and uncertainty to the point where real forest change could be determined with confidence. Several ongoing improvements are expected to reduce error in future nearest-neighbor maps. In model development, each plot will be paired with LandTrendr imagery from the same year of plot measurement, reducing the temporal mismatch from the current maximum of six years down to one year. In addition, information on historical context (disturbance history) available from the LandTrendr time-

series will be incorporated as spatial predictors, which has the potential to greatly increase prediction accuracy (Pflugmacher et al., in press). Although recruitment of older forest through growth and restoration activities is a key objective of the NWFP, small changes in average tree diameter in mid- to late-successional forests are particularly difficult to detect with Landsat imagery (Cohen et al., 1995). The above-mentioned enhancements should improve capabilities to map this kind of forest development.

Lastly, error in the field plot data contributes to an unknown degree to the total error present in the imputed maps. This includes sampling error within plots, which affects how well the sample trees represent the surrounding stand, as well as differences in plot design among the component datasets used in our analysis. Tree tally collected using different plot designs will produce different plot classifications and estimates of landscape proportions of older forest (Williams et al., 2001; Gray, 2003). However, the inventory plot designs and measurement protocols for the primary plot datasets used in our analysis (FIA and CVS) are similar. An analysis by Gray et al. (2009) indicates that FIA and CVS plots produce similar plot-level estimates for several forest attributes in the Oregon Coast Range, including for the OGSI composite variable we used in this paper. Further research is needed to quantify sampling effects on estimates of older forest in other forest ecosystems, and to quantify effects on the imputed maps. The differences among plot designs used in our analyses are another reason we caution against pixel-level interpretation of $k = 1$ nearest neighbor maps.

3.5. Implications for older forest policy

The methods for spatial monitoring of forest conditions presented in this paper provide an unprecedented wealth of information about forest landscape patterns and dynamics over broad regions. The pixel-level data on multiple forest attributes, expressed as continuous variables, can be summarized, post-classified, and re-scaled to address a wide array of forest management and policy issues. This flexibility is perhaps the greatest advantage of maps developed with nearest-neighbor imputation, and in this paper we demonstrated this flexibility using two attributes of older forest. However, the richness and complexity of the data pose new challenges for use of the information by forest managers and policy-makers. It is incumbent on researchers and developers of this information to be as transparent as possible about methods, and to provide useful measures of map uncertainty to guide interpretation and application of the maps. As noted in previous papers (Ohmann and Gregory, 2002; Pierce et al., 2009), GNN maps constructed from regional inventory plots and Landsat imagery are useful for many applications in land management and conservation planning at landscape to regional scales, but should not be expected to be sufficiently reliable for project-scale applications. This is perhaps even more so for maps of forest change derived from GNN maps for two or more points in time.

Controversy has surrounded the conservation and use of older forests in the Pacific Northwest – and in many other parts of the world – for several decades if not longer, and will no doubt continue. Our methods for characterizing forest conditions and dynamics over large regions, and for describing the reliability of the information, should help inform this debate. By providing information comprised of multiple forest attributes as continuous variables, at a moderate spatial resolution, debates over how to define older forest can shift to discussions of which definitions are most appropriate for the stated objectives. We have illustrated how, with the paired LandTrendr/GNN maps, effects of varying the definitions and thresholds on estimates of older forest area can be examined explicitly.

References

Barbour, M., Keeler-Wolf, T., Schoenherr, A.A., 2007. Terrestrial Vegetation of California, third ed. University of California Press, p. 730.

Chen, J.J., Tsai, C.-A., Moon, H., Ahn, H., Young, J.J., Chen, C.-H., 2006. Decision threshold adjustment in class prediction. SAR and QSAR in Environmental Research 17, 337–352.

Cohen, W.B., Spies, T.A., Fiorella, M., 1995. Estimating the age and structure of forests in a multi-ownership landscape of western Oregon, USA. International Journal of Remote Sensing 16, 721–746.

Cohen, W.B., Yang, Z., Kennedy, R., 2010. Detecting trends in forest disturbance and recovery using yearly Landsat time series: 2. TimeSync – tools for calibration and validation. Remote Sensing of Environment 114, 2911–2924.

Crist, E.P., Cicone, R.C., 1984. A physically-based transformation of Thematic Mapper data-the TM tasseled cap. IEEE Transactions on Geoscience and Remote Sensing 22, 256–263.

Daly, C., Halbleib, M., Smith, J.L., Gibson, W.P., Doggett, M.K., Taylor, G.H., Curtis, J., Pasteris, P.P., 2008. Physiographically sensitive mapping of climatological temperature and precipitation across the conterminous United States. International Journal of Climatology 28, 2031–2064.

Duane, M.V., Cohen, W.B., Campbell, J.L., Hudiburg, T., Turner, D.P., Weyermann, D., 2010. Implications of alternative field-sampling designs on Landsat-based mapping of stand age and carbon stocks in Oregon forests. Forest Science 56, 405–416.

Eskelson, B.N.I., Hailemariam, T., LeMay, V., Barrett, T.M., Crookston, N.L., Hudak, A.T., 2009. The roles of nearest neighbor methods in imputing missing data in forest inventory and monitoring databases. Scandinavian Journal of Forest Research 24, 235–246.

Franklin, J.F., Dyrness, C.T., 1988. Natural Vegetation of Oregon and Washington. OSU Press, Oregon State University, Corvallis, Oregon, USA.

Gray, A.N., 2003. Monitoring stand structure in mature coastal Douglas-fir forests: effect of plot size. Forest Ecology and Management 175, 1–16.

Gray, A.N., Monleon, V.J., Spies, T.A., 2009. Characteristics of Old-Growth Forests in the Northern Coast Range of Oregon and Comparison to Surrounding Landscape. General Technical Report PNW-GTR-790.

Hemstrom, M., Spies, T.A., Palmer, C.J., Kiester, R., Teply, J., McDonald, P., Warbington, R., 1998. Late-Successional and Old-Growth Forest Effectiveness Monitoring Plan for the Northwest Forest Plan. General Technical Report PNW-GTR-438.

Kennedy, R.E., Yang, Z., Cohen, W.B., 2010. Detecting trends in forest disturbance and recovery using yearly Landsat time series: 1. LandTrendr – temporal segmentation algorithms. Remote Sensing of Environment 114, 2897–2910.

Kennedy, R.E., Yang, Z., Cohen, W.B., Pfaff, E., Braaten, J., Nelson, P., in press. Spatial and temporal patterns of forest disturbance and within the area of the Northwest Forest Plan. Remote Sensing of Environment.

McRoberts, R.E., Magnussen, S., Tomppo, E.O., Chirici, G., Finley, A.O., 2012. Parametric, bootstrap, and jackknife variance estimators for the k-Nearest Neighbors technique with illustrations using forest inventory and satellite image data. Forest Ecology and Management 272, 3–12.

McRoberts, R.E., Tomppo, E.O., Finley, A.O., Heikkinen, J., 2007. Estimating areal means and variances of forest attributes using the k-Nearest Neighbors technique and satellite imagery. Remote Sensing of Environment 111, 466–480.

McRoberts, R.E., Tomppo, E.O., Naesset, E., 2010. Advances and emerging issues in national forest inventories. Scandinavian Journal of Forest Research 25, 368–381.

Magnussen, S., McRoberts, R.E., Tomppo, E.O., 2010. A resampling variance estimator for the k nearest neighbours technique. Canadian Journal of Forest Research 40, 648–658.

Max, T.A., Schreuder, H.T., Hazard, J.W., Oswald, D.O., Teply, J., Alegria, J., 1996. The Pacific Northwest Region Vegetation Inventory and Monitoring System. Research Papper PNW-RP-493.

Moeur, M., Spies, T.A., Hemstrom, M., Martin, J.R., Alegria, J., Browning, J., Cissel, J., Cohen, W.B., Demeo, T.E., Healey, S., Warbington, R., 2005. Northwest Forest Plan – The first 10 years (1994–2003): Status and Trend of Late-Successional and Old-Growth Forest. General Technical Report PNW-GTR-646.

Moeur, M., Ohmann, J.L., Kennedy, R.E., Cohen, W.B., Gregory, M.J., Yang, Z., Roberts, H.M., Spies, T.A., Fiorella, M., 2011. Northwest Forest Plan – Status and Trends of Late-Successional and Old-Growth Forests from 1994 to 2007. General Technical Report PNW-GTR-853.

Ohmann, J.L., Gregory, M.J., 2002. Predictive mapping of forest composition and structure with direct gradient analysis and nearest neighbor imputation in coastal Oregon, USA. Canadian Journal of Forest Research 32, 725–741.

Ohmann, J.L., Gregory, M.J., Henderson, E.B., Roberts, H.M., 2011. Mapping gradients of community composition with nearest-neighbour imputation: extending plot data for landscape analysis. Journal of Vegetation Science 22, 660–676.

Ohmann, J.L., Gregory, M.J., Spies, T.A., 2007. Influence of environment, disturbance, and ownership on forest vegetation of Coastal Oregon. Ecological Applications 17 (1), 18–33.

Pflugmacher, D., Cohen, W.B., Kennedy, R.E., in press. Remote Sensing of Environment.

Pierce, K.B., Lookingbill, T.R., Urban, D.L., 2005. A simple method for estimating potential relative radiation (PRR) for landscape-scale vegetation analysis. Landscape Ecology 20, 137–147.

Pierce Jr., K.B., Ohmann, J.L., Wimberly, M.C., Gregory, M.J., Fried, J.S., 2009. Mapping wildland fuels and forest structure for land management: a comparison of nearest-neighbor imputation and other methods. Canadian Journal of Forest Research 39, 1901–1916.

Ricker, W.E., 1984. Computation and uses of central trend lines. Canadian Journal of Zoology 62, 1897–1905.

Riemann, R., Wilson, B.T., Lister, A., Parks, S., 2010. An effective assessment protocol for continuous geospatial datasets of forest characteristics using USFS Forest Inventory and Analysis (FIA) data. Remote Sensing of Environment 114, 2337–2352.

Spies, T.A., McComb, B.C., Kennedy, R.S.H., McGrath, M.T., Olsen, K., Pabst, R.J., 2007. Potential effects of forest policies on terrestrial biodiversity in a multi-ownership province. Ecological Applications 17, 48–65.

ter Braak, C.J.F., 1986. Canonical correspondence analysis: a new eigenvector technique for multivariate direct gradient analysis. Ecology 67, 1167–1179.

US Department of Agriculture Forest Service (USFS), 2003. Forest Inventory and Analysis National Core Field Guide, vol. 1. Field Data Collection Procedures for Phase 2 Plots, Version 2.0. Washington, DC.

US Department of Agriculture Forest Service, US Department of the Interior, Bureau of Land Management (USDA USDI), 1994a. Final Supplemental Environmental Impact Statement on Management of Habitat for Late-Successional and Old-Growth Forest Related Species within the Range of the Northern Spotted Owl. Portland, OR.

US Department of Agriculture Forest Service, US Department of the Interior, Bureau of Land Management (USDA USDI), 1994b. Record of Decision for Amendments to Forest Service and Bureau of Land Management Planning Documents within the Range of the Northern Spotted Owl. p. 74 (plus attachment A: standards and guidelines).

Williams, M.S., Schreuder, H.T., Czaplewski, R.L., 2001. Accuracy and efficiency of area classifications based on tree tally. Canadian Journal of Forest Research 31, 556–560.